Quaternary Research **53,** 196–202 (2000)
doi:10.1006/qres.1999.2111, available online at http://www.idealibrary.com on IDEAL®

Speleothem Evidence for Changes in Indian Summer Monsoon Precipitation over the Last ~2300 Years

Rhawn F. Denniston[1] and Luis A. González

Department of Geology, University of Iowa, Iowa City, Iowa 52242

E-mail: rhawn-denniston@uiowa.edu

Yemane Asmerom

Department of Earth and Planetary Science, University of New Mexico, Albuquerque, New Mexico 87131

Ram H. Sharma

Himalayan Climate Centre, Kathmandu, Nepal

and

Mark K. Reagan

Department of Geology, University of Iowa, Iowa City, Iowa 52242

Received March 29, 1999

Speleothems from a well-ventilated dolomitic cave in the Pokhara Valley, central Nepal, preserve a mineralogic record of Indian summer monsoon variability over the past 2300 yr. Annually deposited aragonite layers formed between 2300 and 1500 yr B.P., indicating reduced monsoon precipitation and increased cave aridity, whereas alternating calcite/aragonite laminae deposited after 1500 yr B.P. record elevated summer monsoon precipitation and increased cave humidity. Dense, optically clear calcite layers deposited from 450 ± 5 to 360 ± 20 yr B.P. (1550 to 1640 A.D.) indicate a less-evaporative cave environment and suggest moister and/or cooler conditions, possibly related to climatic change associated with the onset of the Little Ice Age.

Key Words: **speleothem; India; monsoon; Little Ice Age; late Holocene.**

INTRODUCTION

The Indian summer monsoon is driven by development of atmospheric low pressure cells over southern Asia in response to elevated heating of the land surface relative to the Arabian Sea. These pressure gradients draw moist air masses landward during the summer, supplying most of the annual precipitation to India, Nepal, and the southern Himalaya. During the winter, flow patterns are reversed, and cool, dry air dominates over south-central Asia (Gregory, 1989; Clemens *et al.,* 1991). Long-term fluctuations in monsoon intensity are linked to glacial/interglacial cycles and orbital forcing (Duplessey, 1982; Van Campo *et al.,* 1982; Clemens *et al.,* 1991; Overpeck *et al.,* 1996), and several continental climate proxies indicate pronounced shifts in Indian summer monsoon intensity throughout the Holocene (Fig. 1). These include studies of pollen (Liu *et al.,* 1998) and ice chemistry (Yao and Thompson, 1992; Thompson *et al.,* 1997) of the Tibetan Dunde ice cap, pollen and lake sediments from northern (Sharma and Singh, 1974; Mazari *et al.,* 1996) and western India (Bryson and Swain, 1981; Enzel *et al.,* 1999), alluvial sequences from western, eastern, and northeastern India (Williams and Clark, 1984), and multiproxy investigations of Tibetan lakes (Van Campo and Gasse, 1993; Fontes *et al.,* 1996; Hui *et al.,* 1996; Van Campo *et al.,* 1996).

Less-well understood is short-duration late Holocene monsoon variability (Gasse and Derbyshire, 1996; Overpeck *et al.,* 1996). Pollen sequences in northeastern India indicate that cool and dry conditions between ~2000 and 1000 cal yr B.P. were followed by a warmer, wetter interval from ~1000 to 400 cal yr B.P. (Mazari *et al.,* 1996) (Radiocarbon ages from previously reported studies have been converted to cal yr B.P. using the CALIB radiocarbon calibration program; Stuiver and Reimer, 1993). The pollen sequence from Dunde ice cap records wet intervals between 2700 and 2200, 1500 and 800, and 600 and 80 yr B.P. (Liu *et al.,* 1998). Peats from southern India

[1] To whom correspondence should be addressed.

0033-5894/00 $35.00

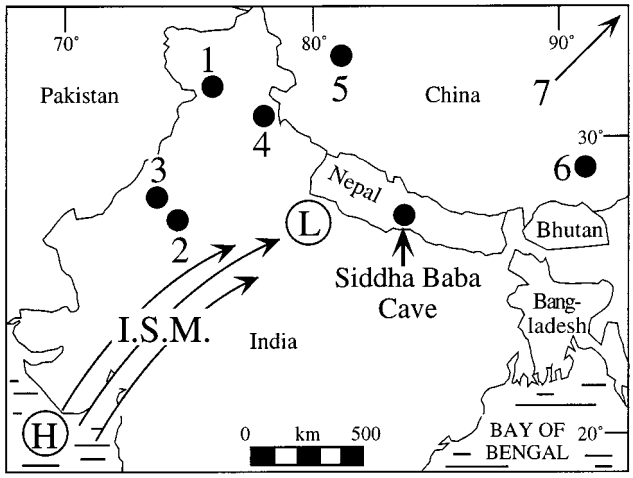

FIG. 1. Map of northern India and adjacent regions showing the position of Siddha Baba cave and other continental paleoclimate records containing evidence of Holocene monsoon activity. 1, Khajiar Lake and Rewalsar Lake; 2, Lake Didwana; 3, Lake Lunkaransar; 4, Takche Lake; 5, Sumxi Co. and Longmu Co.; 6, Qinghai-Xizang Plateau sediments; 7, Dunde ice cap (see text for references). The Indian summer monsoon (I.S.M.) develops in response to the development of low pressure systems (L) over the Tibetan Plateau relative to higher pressures (H) over the Arabian Sea.

(Sukumar *et al.,* 1993) indicate sudden shifts toward wetter conditions at approximately 3000, 1500, and 900 cal yr B.P. Analysis of pollen in alluvial and lake sediments from southwestern China suggest dry and cold conditions from 3200 to 1350 cal yr B.P., mild conditions between 1350 and 300 cal yr B.P., and cold climates again from 300 cal yr B.P. to present (Fu-Bao and Fan, 1987).

While evidence exists for large-scale interrelated climate shifts, including a proposed teleconnection via the East Tropical Jet that links Tibet and northern tropical and subtropical Africa (Van Campo and Gasse, 1993), considerable variability exists in the nature, timing, and lateral extent of monsoon activity. Temporal and/or geographic differences in monsoon character are not unexpected and have been described from historical records (Gregory, 1989). In addition, regional paleoclimatic records also illustrate this variability. For example, Lunkaransar Lake and Didwana Lake in Rajasthan, northwestern India, underwent large-scale fluctuations in water levels throughout the Holocene. However, Didwana Lake decreased significantly in size during the first 60% of the Holocene while Lunkaransar Lake did not undergo such a clear decline. In addition, Lunkaransar Lake desiccated at ~5000 cal yr B.P. (Enzel *et al.,* 1999), whereas Didwana Lake became dry at ~2500 cal yr B.P. (Bryson and Swain, 1981).

The use of speleothem mineralogy for paleoclimatic reconstruction has been previously proposed (Bar-Matthews *et al.,* 1991; Railsback *et al.,* 1994; Genty and Quinif, 1996). Carbonate rocks host numerous caves across much of central Nepal (Baeumler and Gebauer, 1992); thus, speleothems provide excellent geographic coverage of an area with limited paleoclimatic records. Here we present a precisely dated, high-resolution mineralogic record from stalagmites that preserves Indian monsoon variability during the last ~2300 years. Two speleothems, SB-18 and SB-19, were collected from Siddha Baba cave near the town of Kheireni in the Seti River Valley of the Pokhara Valley, central Nepal (lat. is 27°59′N, long. is 84°04′E, elevation is ~2000 m), a region where the climate is dominated by the Indian summer monsoon (Fig. 1). The entrance to Siddha Baba has an area of ~4 m^2 and is located 10 m above a small stream. The cave is formed in the lower Paleozoic Dhading dolomite and is composed of two, quasi-circular rooms, the first of which is equal in elevation to the entrance and is approximately 40 m^2. A second, larger room is entered by ascending 4 m through a 1-m^2 subvertical passage. All areas of the cave were dry when visited in December, 1995, only 4 months after the termination of the summer monsoon, suggesting that the rocks hosting the cave do not act as significant reservoirs of summer monsoon moisture, and that infiltration to the cave is strongly seasonal.

ANALYTICAL METHODS

The stalagmites were sawed in half along the long axes of deposition and were polished. Samples for dating were drilled from along the vertical growth axis using a modified dental drill. Sample sizes approached 200 mg for thermal ionization mass spectrometry (TIMS) and ~800 mg for alpha spectrometry. Uranium–thorium TIMS analysis was performed at the Radiogenic Isotope Laboratory at the University of New Mexico. Samples were dissolved in HNO_3 and then spiked with ^{229}Th, ^{233}U, and ^{236}U. Chemical separation was modified from Chen *et al.* (1986). The U and Th were measured on a Micromass Sector 54 thermal ionization mass spectrometer with a high-abundance sensitivity filter. All isotopes of interest were measured on an ion-counting Daly multiplier with abundance sensitivity in the range of 20 ppb at one mass distance in the mass range of U and Th, requiring very little background correction, even for samples with large ^{232}Th content. Multiplier dark noise was about 0.12 counts per second. The NBL-112 U standard was measured during the course of this study and remained in the range of 0.1% of the accepted $^{234}U/^{238}U$ ratio.

Alpha spectrometry was performed at the University of Iowa. Samples were dissolved and spiked with ^{228}Th and ^{232}U. Chemical separation techniques were modified from Chen *et al.* (1986). U and Th were electroplated on stainless steel disks using ammonium chloride and ammonium oxalate plating solutions and were counted for 4 to 8 days depending on activity levels. Isotopic compositions determined by alpha spectrometry agree well with isotopic ratios obtained with mass spectrometry (Table 1). All U-series ages are reported with 2σ uncertainties.

TABLE 1
Uranium and Thorium Isotopic Ratios and $^{230}Th/^{234}U$ Ages

Sample (mineral)[a]	mm from bottom[b]	^{238}U ($\mu g/g$)	^{232}Th (ng/g)	$\delta^{234}U$[c,d] measured	$^{230}Th/^{238}U$ activity	$^{230}Th/^{232}Th$ atomic	Age[e]	Dating method
SB-18 (a)	460	12.4	0.30	−58.5 (14)	3.14×10^{-3} (20)	2.16×10^{-3} (17)	360 (20)	TIMS
SB-18 (a)	440	21.4	1.14	−56.3 (32)	3.92×10^{-3} (5)	1.21×10^{-3} (2)	450 (7)	TIMS
SB-18 (a)	182	6.70	b.d.[f]	−39.3 (11)	1.42×10^{-2} (21)	b.d.	1590 (240)	alpha
SB-18 (a)	135	12.6	b.d.	−8.40 (20)	1.71×10^{-2} (23)	b.d.	1890 (250)	alpha
SB-18 (a)	2	16.8	b.d.	−32.6 (65)	2.32×10^{-2} (20)	b.d.	2640 (300)	alpha
SB-19 (l)	321	6.94	15.84	−76.9 (20)	2.52×10^{-3} (9)	1.82×10^{-5} (6)	230 (30)	TIMS
SB-19 (a)	307	6.73	b.d.	−35.8 (30)	1.10×10^{-2} (26)	b.d.	1240 (310)	alpha
SB-19 (l)	283	2.93	20.67	−42.2 (25)	1.67×10^{-2} (5)	3.89×10^{-5} (13)	1490 (120)	TIMS
SB-19 (a)	277	8.67	1.28	−41.4 (15)	1.32×10^{-2} (2)	1.48×10^{-3} (3)	1510 (20)	TIMS
SB-19 (a)	50	5.21	b.d.	−43.0 (12)	1.71×10^{-2} (9)	b.d.	1960 (320)	alpha
SB-19 (l)	5	8.51	8.40	−19.4 (19)	2.07×10^{-2} (1)	3.45×10^{-4} (2)	2290 (20)	TIMS

[a] Mineralogy abbreviations: a, aragonite; c, calcite; 1, aragonite/calcite laminae.

[b] Total length of SB-18 = 512 mm; SB-19 = 331 mm.

[c] $\delta^{234}U_{\text{measured}} = [(^{234}U/^{238}U)_{\text{measured}}/(^{234}U/^{238}U)_{\text{eq}} - 1] \times 10^3$, where $(^{234}U/^{238}U)_{\text{eq}}$ is the secular equilibrium atomic ratio: $\lambda_{238}/\lambda_{234} = 5.472 \times 10^{-5}$.

[d] Values in parentheses represent 2σ errors in the last significant figure. In all cases, age uncertainties are equal to or less than the number of annual bands sampled for dating.

[e] Unsupported ^{230}Th was subtracted using an initial $^{230}Th/^{232}Th$ ratio of 8.5×10^{-6} ($\pm 2.125 \times 10^{-6}$). This value was obtained by correcting SB-19-283 in order to place it in correct stratigraphic sequence relative to the precisely dated SB-19-277 which underlies it.

[f] b.d., below detection using alpha spectrometry.

Mineral phases were identified using optical, chemical (Feigel's solution) (Friedman, 1959), and X-ray diffraction (XRD) techniques. XRD analyses were performed on ~3 mg of powder using a Philips APD 3720 X-ray diffractometer and were used for qualitative assessment of speleothem mineralogy.

CLIMATIC CONTROLS ON SPELEOTHEM MINERALOGY

Siddha Baba stalagmites are largely aragonite. Aragonite speleothems occur in caves associated with dolomite (González and Lohmann, 1988) and are linked to arid cave conditions (Murray, 1954; Thrailkill, 1971; Bar-Matthews *et al.,* 1991; Railsback *et al.,* 1994). Dissolution of dolomite bedrock produces drip waters with initial Mg/Ca ratios ranging from ~0.6 to 0.9 (depending on the stoichiometry of the host dolomite) (Thrailkill, 1976; Evens *et al.,* 1986; González and Lohmann, 1988; Turin, 1995) and can exceed 1.0 in response to preferential removal of Ca^{2+} during precipitation of calcium carbonate mineral phases (e.g., along stalactites or in the vadose zone overlying the cave) (Möller and Kubanek, 1976; González and Lohmann, 1988). Numerous studies have demonstrated that Mg inhibits calcite crystallization while not affecting aragonite crystallization (e.g., Bischoff, 1968; Berner, 1975; Fernández-Díaz *et al.,* 1996; Deleuze and Brantley, 1997).

Recent work on speleothems, springs, and hydrothermal systems (e.g., travertines) has demonstrated that at temperatures consistent with cave drip waters, Mg/Ca molar ratios in excess of ~1.0 are required to precipitate aragonite (González and Lohmann, 1988; Folk, 1994; Morse *et al.,* 1997). In order for aragonite to become the dominant mineral phase, however, higher Mg/Ca molar ratios are required; Möller and Kubanek (1976) report ratios of ~1.5, González and Lohmann (1988) report ratios of 2.5, and Fischbeck and Müller (1971) found that a ratio of 4.4 is necessary. Only at temperatures in excess of ~40°C is aragonite favored over calcite at low Mg/Ca ratios (Folk, 1994; Deleuze and Brantley, 1997). In addition, evaporation increases the degree of saturation of the solution with respect to calcite, thus raising calcite precipitation rates and accelerating removal of Ca^{2+} from solution (Railsback *et al.,* 1994). However, while Ca^{2+} concentrations decrease, Mg^{2+} is concentrated in the remaining fluid. Thus, under evaporative conditions, Mg/Ca ratios increase more rapidly than during humid (less evaporative) conditions and aragonite tends to be favored (González and Lohmann, 1988; Bar-Matthews *et al.,* 1991; Railsback *et al.,* 1994).

Crystallization rates also affect the precipitation of aragonite and calcite. Growth rate is a function of degree of supersaturation (Chernov, 1984; Morse and Mackenzie, 1990; Fernández-Díaz *et al.,* 1996), and as the supply of CO_3^{2-} determines the degree of calcite supersaturation in many natural environments, when CO_3^{2-} is readily available the solution is more highly saturated and often favors aragonite as the predominant calcium carbonate mineral phase (Given and Wilkinson, 1985; Fernández-Díaz *et al.,* 1996). Because infiltration rate can impact drip-water chemistry (Bar-Matthews *et al.,* 1996; Baker *et al.,* 1997), shifts in cave hydrology can affect speleothem mineralogy. In addition, sudden loss of CO_2

can result in instantaneous aragonite supersaturation so that aragonite potentially can precipitate from non-Mg-bearing fluids (Chafetz *et al*., 1991). At very high saturation states, growth rates can be sufficiently elevated so as to override the inhibitory effects of Mg^{2+} on calcite crystallization (Fernández-Díaz *et al*., 1996). Thus, under extremely high precipitation rates, Mg–calcite (6 to 10 mol% $MgCO_3$) or high-Mg–calcite (>10 mol% $MgCO_3$) can crystallize.

In monsoonal climates, calcite crystallization is favored in many speleothems during the wet season because cave humidity is increased in response both to elevated infiltration and to less evaporative loss to the outside atmosphere, as well as to potentially lower calcite saturation states. Aragonite is favored during relatively dry intermonsoon months when the cave becomes more evaporative and slower infiltration rates allow for potentially higher calcite saturation states (Railsback *et al*., 1994). A decrease in the intensity of precipitation during the monsoon period could therefore result in aragonite precipitation throughout the entire year.

RESULTS

The stalagmites were dated with precision 4 to 10 times better than radiocarbon or ice layer counting dates of similar age, or similarly sized calcite samples, because aragonite incorporates U more readily than does calcite; we observed U concentrations as high as 21 ppm. In addition, throughout the majority of the aragonitic portions of these speleothems, numbers of visible growth bands agree to within the error of radiometric dates, demonstrating that they are annually deposited—likely in response to monsoon cycles. Annual layering has been previously identified from speleothems in temperate regions based on annual laminae (Broecker and Olson, 1960; Genty and Quinif, 1996) and fluorescent banding (Baker *et al*., 1993) and from monsoonal climates based on calcite–aragonite mineralogy (Railsback *et al*., 1994). Age determinations are limited in the more calcite-rich portions of SB-19 (and to a much lesser degree, SB-18) by abundant illuviated clays with poorly constrained $^{230}Th/^{232}Th$ ratios.

SB-19 is composed of annually banded aragonite ranging in age from 1500 to 2300 yr B.P. Laminae were deposited in cycles, probably associated with the summer monsoon. A sharp, easily recognized transition from laminae composed exclusively of aragonite to laminae defined by distinct alternating layers of calcite and aragonite exists at 1500 yr B.P. (Figs. 2 and 3). No evidence for interrupted growth or recrystallization is observed at the aragonite to calcite/aragonite transition, either in hand samples or in thin sections. A small amount of calcite is visible below the transition from banded aragonite and calcite/aragonite laminae.

SB-18 is characterized by a complex growth geometry resulting from numerous changes in drip position. The last 1500 yr of SB-18 is more aragonitic than SB-19, and as a result, growth rates, and temporal resolution, are higher than in SB-19. Three dense, optically clear calcite layers exist in the upper 20% of SB-18 at 443 to 453, 455 to 457, and 460 to 462 mm. Two mass spectrometry dates bracket this part of the stalagmite and place these calcite intervals between 450 and 360 yr B.P. (1550 to 1640 A.D.). It is extremely difficult to assign tight age constraints to specific calcite laminae in SB-19, however, because the same time interval is compressed into about 10% of the distance in the vertical growth direction, and high ^{232}Th abundances limit the precision available by U/Th dating techniques. X-ray diffraction analysis demonstrates that the calcite portions of these speleothems are low-Mg calcite (<5 mol% $MgCO_3$).

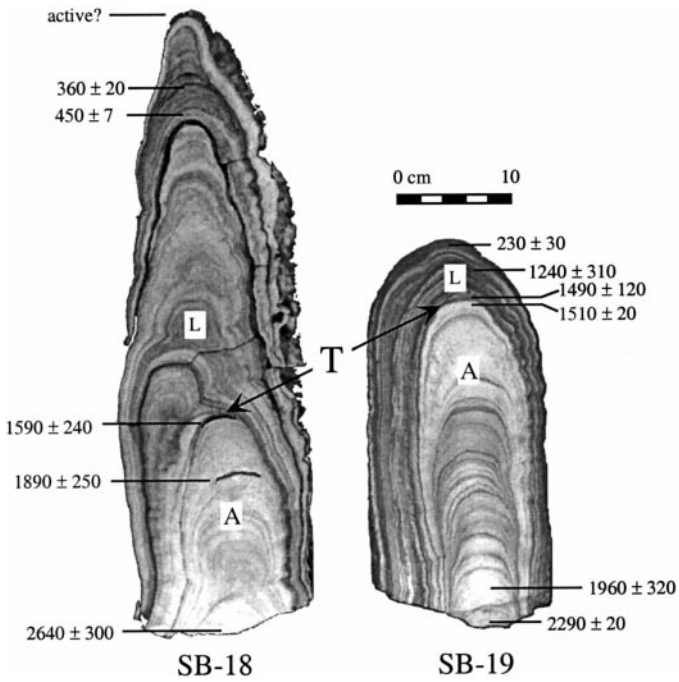

FIG. 2. Cross-sectional view of SB-18 (left) and SB-19 (right) demonstrating mineralogical changes and radiometric ages in years B.P. T, transition between aragonite (A) and calcite/aragonite laminae (L).

DISCUSSION

Between ~2300 and 1500 yr B.P., Siddha Baba speleothems formed almost entirely as aragonite, indicating reduced drip rates and/or arid conditions throughout the year. The overall lack of alternating calcite laminae suggests that summer monsoon precipitation was diminished relative to the period after 1500 yr B.P. Sporadic calcite layers are present during this interval and may record anomalously wet summer monsoons in a period of overall elevated aridity. The mineralogic transition about 1500 yr B.P. records increased summer monsoon precipitation and heightened infiltration into Siddha Baba that elevated cave humidity during the monsoon season and dimin-

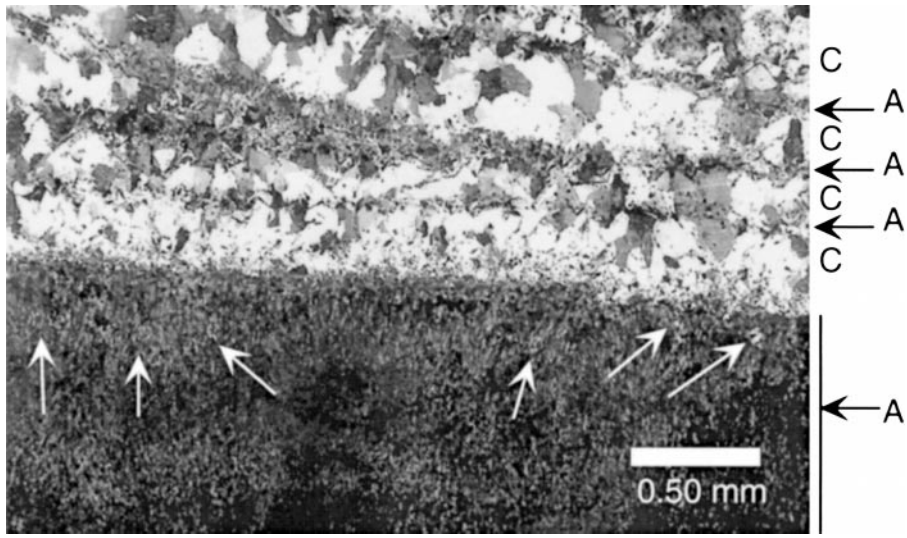

FIG. 3. Photomicrograph of SB-19 showing the transition from banded aragonite (bottom) to alternating calcite (C) and aragonite (A) laminae (top). Field of view is 3.2 mm × 2.1 mm. Arrows denote calcite intergrown with aragonite prior to primary mineralogic transition at 1500 yr B.P.

ished evaporation to the point that calcite crystallized from cave drip water. The sharp contact between mineralogic domains suggests that summer monsoon precipitation increased suddenly at ~1500 yr B.P. The association of illuviated clays with calcite/aragonite laminae also argues for rapid changes in infiltration ate. However, it also is possible that infiltration rates and/or cave humidity were increasing gradually over a long time prior to 1500 yr B.P., but conditions appropriate for formation of calcite were not reached until 1500 yr B.P. Nonclimatic factors that could also have influenced cave mineralogy, such as changes in infiltration hydraulics or cave geometry (e.g., closing off of the cave atmosphere by landslide blockage of the cave entrance), are not likely because (1) aragonite continued to crystallize during the relatively dry intermonsoon months and (2) illuviated clays are rare in aragonitic layers but are abundant in calcite/aragonite laminae, suggesting more rapid water flux through the overlying soil and bedrock.

During the late Holocene, monsoon circulation responded to climatic changes, including Neoglacial cooling (Liu *et al.,* 1998). Pollen and oxygen isotope studies of the Dunde ice cap in Tibet suggest that decreased summer temperatures played a more significant role than increased summer precipitation in elevating effective moisture during the late Holocene (Thompson *et al.,* 1997; Liu *et al.,* 1998). Our data indicate that in the Pokhara Valley, the last 1500 years witnessed greater monsoon precipitation than the preceding millennium, with wetter conditions resulting from a stronger summer monsoon. Pollen evidence from the Dunde ice cap also suggests that during the Little Ice Age (1660–1910 A.D.), the Tibetan Plateau was characterized by cool and humid conditions (Liu *et al.,* 1998). Our findings of dense calcite beginning at 450 ± 5 yr B.P. (1550 A.D.) argue for cave conditions that were sufficiently cool and/or moist to suppress evaporation and allow calcite crystallization all year. This supports a climatic scenario similar to that proposed by Liu *et al*. (1998), but these speleothem data indicate that Little Ice Age climate change apparently began ~100 yr earlier in the Pokhara Valley than at the Dunde ice cap.

CONCLUSIONS

Changes in speleothem mineralogy record shifts in the intensity of the Indian summer monsoon during the late Holocene. While the forcing mechanisms behind these changes remain unclear, gross similarity exists between regional climate records that suggest a shift toward more humid conditions ~1500 yr B.P. Well-developed karst across northern India and the southern Himalaya may allow increased geographic coverage of monsoon variability as recorded in speleothems, and thus may help us assess the synchrony of changes in summer monsoon precipitation on a regional scale.

ACKNOWLEDGMENTS

The authors thank Dr. C.K. Sharma, Nepal Royal Academy of Science, and Dr. S. Adhikiry, Himalayan Climate Centre, for their generous assistance in Nepal. This research was funded, in part, by grants from the Geological Society of America, the Richmond Area Speleological Society, the Cave Research Foundation, the National Speleological Society, and the University of Iowa College of Liberal Arts (all to R.D.).

REFERENCES

Baker, A., Smart, P. L., Edwards, R. L., and Richards, D. A. (1993). Annual growth banding in a cave stalagmite. *Nature* **364,** 518–520.

Baeumler, G., and Gebauer, H. D. (1992). Siddha-Gupha, the deepest cave in Nepal. *Mitteilungen—Verband Deutscher Hoehlen und Karstforscher* **38,** 38.

Baker, A., Ito, E., Smart, P. L., and McEwan, R. F. (1997). Elevated and variable values of ^{13}C in speleothems in a British cave system. *Chemical Geology* **136,** 263–270.

Bar-Matthews, M., Matthews, A., and Ayalon, A. (1991). Environmental controls on speleothem mineralogy in a karstic dolomitic terrain (Soreq Cave, Israel). *Journal of Geology* **99,** 189–207.

Bar-Matthews, M., Ayalon, A., Matthews, A., Sass, E., and Halicz, L. (1996). Carbon and oxygen isotope study of the active water–carbonate system in a karstic Mediterranean cave: Implications for paleoclimate research in semi-arid regions. *Geochimica et Cosmochimica Acta* **60,** 337–347.

Berner, R. A. (1975). The role of magnesium in the crystal growth of calcite and aragonite from seawater. *Geochimica et Cosmochimica Acta* **39,** 489–504.

Bischoff, J. L. (1968). Kinetics of calcite nucleation: Magnesium ion inhibition and ionic strength catalysis. *Journal of Geophysical Research* **73,** 3315–3322.

Broecker, W. S., and Olson, E. A. (1960). Radiocarbon measurements and annual banding in cave formations. *Nature* **185,** 93–94.

Bryson, R. A., and Swain, A. M. (1981). Holocene variations of monsoon rainfall in Rajasthan. *Quaternary Research* **16,** 125–145.

Chafetz, H. S., Rush, P. F., and Utech, N. M. (1991). Microenvironmental controls on mineralogy and habit of CaCO3 precipitates: An example from an active travertine system. *Sedimentology* **38,** 107–126.

Chen, J., Edwards, L., and Wasserburg, W. (1986). ^{238}U, ^{234}U, and ^{232}Th in seawater. *Earth and Planetary Science Letters* **80,** 241–251.

Chernov, A. A. (1984). "Modern Crystallography III. Crystal Growth." Berlin, Springer-Verlag, 517 pp.

Clemens, S., Prell, W., Murray, D., Shimmield, G., and Weedon, G. (1991). Forcing mechanisms of the Indian Ocean monsoon. *Nature* **353,** 720–725.

Deleuze, M., and Brantley, S. L. (1997). Inhibition of calcite crystal growth by Mg^{2+} at 100°C and 100 bars: Influence of growth regime. *Geochimica et Cosmochimica Acta* **61,** 1475–1485.

Duplessey, J. C. (1982). Glacial to interglacial contrasts in the northern Indian Ocean. *Nature* **295,** 494–498.

Enzel, Y., Ely, L. L., Mishra, S., Ramesh, R., Amit, R., Lazar, B., Rajaguru, S. N., Baker, V. R., and Sandler, A. (1999). High-resolution Holocene environmental changes in the Thar Desert, northwestern India. *Science* **284,** 125–128.

Even, H., Carmi, I., Magaritz, M., and Gerson, R. (1986). Timing the transport of water through the upper vadose zone in a karstic system above a cave in Israel. *Earth Surfaces Processes and Landforms* **11,** 181–191.

Fernández-Díaz, L., Putnis, A., Prieto, M., and Putnis, C. V. (1996). The role of magnesium in the crystallization of calcite and aragonite in a porous medium. *Journal of Sedimentary Research* **66,** 482–491.

Fischbeck, R., and Müller, G. (1971). Monohydrocalcite, hydromagnesite, nesquehonite, dolomite, aragonite, and calcite in speleothems of the Fränkische Schwiz, western Germany. *Contributions to Mineralogy and Petrology* **33,** 87–92.

Folk, R. L. (1994). Interaction between bacteria, nannobacteria, and mineral precipitation in hot springs of central Italy. *Géographie Physique et Quaternaire* **48,** 233–246.

Fontes, J.-C., Gasse, F., and Gibert, E. (1996). Holocene environmental changes in Bangong Co basin (Western Tibet). Part 1: Chronology and stable isotopes of carbonates of a Holocene lacustrine core. *Palaeogeography, Palaeoclimatology, Palaeoecology* **120,** 25–47.

Friedman, G. M. (1959). Identification of carbonate minerals by staining methods. *Journal of Sedimentary Petrology* **29,** 87–97.

Fu-Bao, W., and Fan, C. Y. (1987). Climatic changes in the Qinghai-Xizang (Tibetan) region of China during the Holocene. *Quaternary Research* **28,** 50–60.

Gasse, F., and Derbyshire, E. (1996). Environmental changes in the Tibetan Plateau and surrounding areas—Preface. *Palaeogeography, Palaeoclimatology, Palaeoecology* **120,** 1–3.

Genty, D., and Quinif, Y. (1996). Annually laminated sequences in the internal structure of some Belgian stalagmites—Importance for paleoclimatology. *Journal of Sedimentary Research* **66,** 275–288.

Given, R. K., and Wilkinson, B. H. (1985). Kinetic control of morphology, composition, and mineralogy of abiotic sedimentary carbonates. *Journal of Sedimentary Petrology* **55,** 109–119.

González, L. A., and Lohmann, K. C. (1988). Controls on mineralogy and composition of spelean carbonates: Carlsbad Caverns, New Mexico. *In* "Paleokurt" (N. P. James and P. W. Choquette, Eds.), pp. 81–101. Kingston, Ontario.

Gregory, S. (1989). Macro-regional definition and characteristics of Indian summer monsoon rainfall, 1871–1985. *International Journal of Climatology* **9,** 465–483.

Hui, F., Gasse, F., Huc, A., Yuanfang, L., Sifeddine, A., and Soulie-Marsche, I. (1996). Holocene environmental changes in Bangong Co basin (Western Tibet). Part 3: Biogenic remains. *Palaeogeography, Palaeoclimatology, Palaeoecology* **120,** 65–78.

Liu, K.-B., Yao, Z., and Thompson, L. G. (1998). A pollen record of Holocene climatic changes from the Dunde ice cap, Qinghai-Tibetan Plateau. *Geology* **26,** 135–138.

Mazari, R. K., Bagati, T. N., Chauhan, M. S., and Rajagopalan, G. (1996). Palaeoclimatic record of last 2000 years in trans-Himalayan Lahaul-Spiti region. *In* "Paleoclimate and Environmental Variability in Austral-Asian Transect during the Past 2000 Years, Proceedings, IGBP-PAGES/PEP II Symposium, Nagoya, Japan," pp. 262–269.

Möller, P., and Kubanek, F. (1976). Role of magnesium in nucleation processes in calcite, aragonite and dolomite—A review. *Neues Jahrbuch fuer Mineralogie Abhandlungen* **126,** 199–220.

Morse, J. W., Wang, Q., and Tsio, M. Y. (1997). Influences of temperature and Mg:Ca ratio on $CaCO_3$ precipitates from seawater. *Geology* **25,** 85–87.

Morse, J. W., and Mackenzie, F. T. (1990). "Geochemistry of Sedimentary Carbonates." Elsevier, Amsterdam, 707 pp.

Murray, J. W. (1954). The deposition of calcite and aragonite in caves. *Journal of Geology* **62,** 481–492.

Overpeck, J., Anderson, D., Trumbore, S., and Prell, W. (1996). The southwest Indian Monsoon over the last 18,000 years. *Climate Dynamics* **12,** 213–225.

Railsback, L. B., Brook, G. A., Chen, J., Kalin, R., and Fleisher, C. J. (1994). Environmental controls on the petrology of a late Holocene speleothem from Botswana with annual layers of aragonite and calcite. *Journal of Sedimentary Research* **A64,** 147–155.

Sharma, C., and Singh, G. (1974). Studies in the late-Quaternary vegetational history of Himachal Pradesh: 1, Khajiar Lake. *The Palaeobotanist* **21,** 144–162.

Stuiver, M., and Reimer, P. J. (1993). Extended ^{14}C database and revised CALIB 3.0 ^{14}C age calibration program. *Radiocarbon* **35,** 215–230.

Sukumar, R., Ramesh, R., Pant, R. K., and Rajagopalan, G. (1993). A $\delta^{13}C$ record of late Quaternary climate change from tropical peats in southern India. *Nature* **364,** 703–706.

Thompson, L. G., Yao, T., Davis, M. E., Henderson, K. A., Mosley-Thompson, E., Lin, P.-N., Beer, J., Synal, H.-A., Cole-Dai, J., and Bolzan, J. F. (1997). Tropical climate instability: The last glacial cycle from a Qinghai-Tibetan ice core. *Science* **276,** 1821–1825.

Thrailkill, J. (1971). Carbonate deposition in Carlsbad Caverns. *Journal of Geology* **79,** 683–695.

Thrailkill, J. (1976). "Studies and Excavation of Limestone Caves and the Deposition of Speleothems." Unpublished Ph.D. dissertation, Princeton University, pp. 193.

Turin, H. J., and Plummer, M. A. (1995). Geochemistry of Lechuguilla Cave pool water. *Geological Society of America Abstracts with Programs* **27,** A-95.

Van Campo, E., Cour, P., and Sixuan, H. (1996). Holocene environmental changes in Bangong Co. Basin (western Tibet): Part 2, The pollen record. *Palaeogeography, Palaeoclimatology, Palaeoecology* **120,** 49–63.

Van Campo, E., Duplessey, J. C., and Rissignol-Strick, M. (1982). Climatic conditions deducted from a 150-kyr oxygen isotope–pollen record from the Arabian Sea. *Nature* **296,** 56–59.

Van Campo, E., and Gasses, F. (1993). Pollen- and diatom-inferred climatic and hydrologic changes in Sumxi Co. Basin (western Tibet) since 13,000 yr B.P. *Quaternary Research* **39,** 300–313.

Williams, M. A. J., and Clark, M. F. (1984). Late Quaternary environments in north-central India. *Nature* **308,** 633–635.

Yao, T., and Thompson, L. G. (1992). Trends and features of climatic changes in past 5000 years recorded by the Dunde ice core. *Annals of Glaciology* **16,** 21–24.